Front. Earth Sci. 2020, 14(4): 770–782
https://doi.org/10.1007/s11707-020-0831-3

RESEARCH ARTICLE

Natural fractures within unconventional reservoirs of Linxing Block, eastern Ordos Basin, central China

Wei JU (✉)[1,2], Jian SHEN[1,2], Chao LI[2], Kun YU[3], Hui YANG[2]

1 Key Laboratory of Coalbed Methane Resources and Reservoir Formation Process, Ministry of Education, China University of Mining and Technology, Xuzhou 221008, China
2 School of Resources and Geosciences, China University of Mining and Technology, Xuzhou 221116, China
3 Key Laboratory of Computational Geodynamics, College of Earth and Planetary Sciences, University of Chinese Academy of Sciences, Beijing 100049, China

Abstract Unconventional reservoirs are generally characterized by low matrix porosity and permeability, in which natural fractures are important factors for gas production. In this study, we analyzed characteristics of natural fractures, and their influencing factors based on observations from outcrops, cores and image logs. The orientations of natural fractures were mainly in the ~N-S, WNW-ESE and NE-SW directions with relatively high fracture dip angles. Fracture densities were calculated based on fracture measurements within cores, indicating that natural fractures were not well-developed in the Benxi-Upper Shihezi Formations of Linxing Block. The majority of natural fractures were open fractures and unfilled. According to the characteristics of fracture sets and tectonic evolution of the study area, natural fractures in the Linxing Block were mainly formed in the Yanshanian and Himalayan periods. The lithology and layer thickness influenced the development of natural fractures, and more natural fractures were generated in carbonate rocks and thin layers in the study area. In addition, in the Linxing Block, natural fractures with ~N-S-trending strikes contributed little to the overall subsurface fluid flow under the present-day stress state. These study results provide a geological basis for gas exploration and development in the Linxing unconventional reservoirs of Ordos Basin.

Keywords natural fracture, unconventional reservoir, Linxing region, influencing factors, Ordos Basin

1 Introduction

Typically, natural gas produced from shales, tight sandstones and carbonates, coal seams, etc., has been classed under unconventional gas, whose production process usually requires stimulation by horizontal drilling coupled with hydraulic fracturing due to the relatively low matrix porosity and permeability in the gas-bearing formations (Olson et al., 2009; Speight, 2019; Bhandakkar et al., 2020). Recently, studies on unconventional gas development have focused on effective fracturing methods; however, in fact, the presence of natural fractures at different scales (micro-, meso-, or macro-scale) and in different types of reservoirs (shale, tight sandstone/carbonate, or coal reservoir) may also greatly influence the exploration and development of unconventional gas (Aydin, 2000; Zeng and Li, 2009; Gale et al., 2014; Ju and Sun, 2016; McGinnis et al., 2017). In addition, natural fractures can also play a critical role during the gas production process through their interactions with hydraulically induced fractures (Dahi-Taleghani and Olson, 2011; Wu and Olson, 2016; Siddhamshetty et al., 2020). Hydraulic fracturing can create new fractures, and increase the size, connectivity, and conducitivity of natural fractures (Bhandakkar et al., 2020). Overall, natural fractures can not only serve as important spaces for storage of hydrocarbons and fluid-flow pathways and enhance the reservoir permeability, but also largely influence hydraulic fracturing. Therefore, understanding where natural fractures are open and capable of transmitting fluid, and knowledge of controlling factors for natural fracture development and distribution are important for unconventional gas exploration and development.

In geology, a fracture is once defined as any discontinuity within rocks where there is no cohesion due to brittle

Received April 12, 2020; accepted July 31, 2020

E-mail: wju@cumt.edu.cn

deformation (Hancock, 1985; Fossen, 2010); however, if minerals deposit within it, a fracture will have cohesion. The variable cohesion of natural fractures is one of the principal ways they interact with hydraulic fractures (e.g., Dahi-Taleghani and Olson, 2011). Many studies have been carried out on natural fractures from geological and reservoir engineering perspectives, e.g., curvature analysis method (Hennings et al., 2000), seismic-based techniques (Hall et al., 2002), geomechanical modeling (Ju et al., 2019), etc. Factors that influence natural fracture development and distribution include tectonic stress field, bed thickness, lithology, mineral composition, mechanical properties, presence of folds and faults, dissolution differences, thermal shrinkage, etc. (e.g., Narr, 1991; Harstad et al., 1995; Hennings et al., 2000; Nelson, 2001; Gale et al., 2007, 2014; Laubach et al., 2009; Olson et al., 2009; Zeng and Li, 2009; Weniger et al., 2016; McGinnis et al., 2017; Ju et al., 2018 and 2019). Even a tiny extensional strain (10^{-4} order) could result in substantial fracture growth (Olson et al., 2009). Hence, understanding those controlling factors for natural fractures well will help guide the prediction of fracture distribution and further hydrocarbon production.

The Linxing Block of eastern Ordos Basin is an important region with large volumes of unconventional gas in China. The geochemical characteristics, physical properties, pore pressure, sequence framework, paleotectonic stress field and present-day *in-situ* stress state of the gas-bearing formations in the Linxing Block have been investigated for a better understanding of the geological conditions and gas production (Li et al., 2016; Ju et al., 2017; Shen et al., 2017; Gao et al., 2018). However, until now, no studies have been focused and carried out on natural fractures within those gas-bearing formations in the Linxing Block, though they are extremely important for unconventional gas production.

Therefore, in this study, characteristics and controlling factors for natural fractures in the Linxing unconventional gas reservoirs were systematically described and analyzed based on analogous outcrop, cores, and borehole image logs. Moreover, the genesis for natural fractures and coupling effects of present-day *in-situ* stress state and pore pressure on natural fractures were also discussed. This study provides an example of natural fracture characterization and indicates the contributions of natural fractures to unconventional gas productions in the Linxing Block of eastern Ordos Basin.

2 Geologic setting

The Ordos Basin, situated in the western part of the North China Craton (Zhao et al., 2005; Fig.1), is a typical intracontinental basin with a complex tectonic-sedimentary history (Zhao et al., 1996; Liu et al., 2009; Ju et al., 2020). The bottom of the basin is a unified crystalline basement

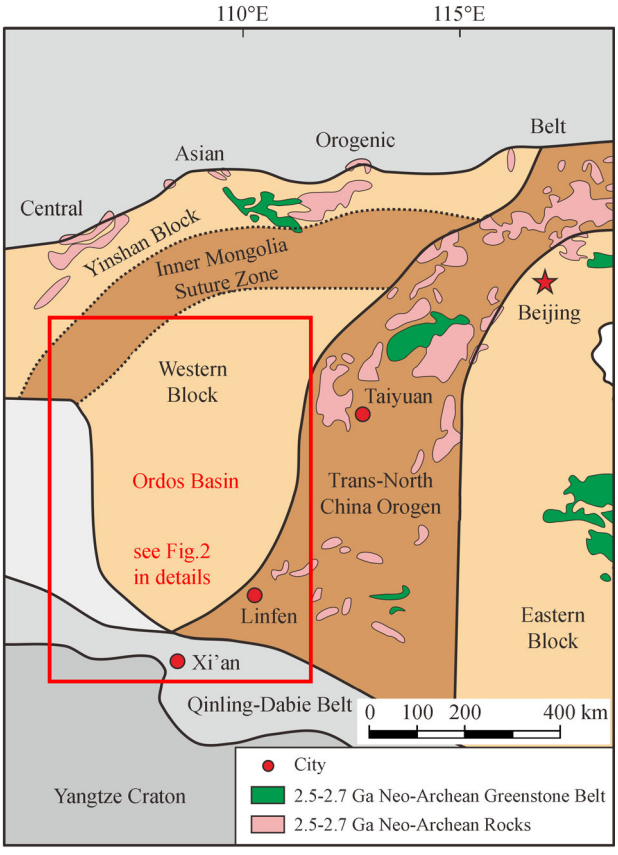

Fig. 1 Generalized tectonic map of the North China Craton (after Zhao et al. (2005)).

formed during the Early Proterozoic, and the sediment cover of the basin started from the Middle to Late Proterozoic. The entire basin began a transitional period from marine to continental sedimentation during the Late Carboniferous, and since then, it experienced the Late Paleozoic littoral plain stage, Mesozoic continental basin stage, and Cenozoic peripheral faulted basin stage (Yang et al., 2005). Influenced by the Yanshanian and Himalayan movements, the basin has been uplifted and subjected to erosion since the Late Cretaceous. Currently, the present-day geomorphology indicates that the central part of the Ordos Basin is tectonically stable; whereas the margins have undergone strong deformations, resulting in structural complexity (Liu et al., 2009; Ju et al., 2015; Fig.2).

The Linxing Block is located in the eastern Ordos Basin (Fig.2). The main gas-bearing layers within this block are the Benxi, Taiyuan, Shanxi, Lower Shihezi, and Upper Shihezi Formations (Fig.3), which are deposited in a tidal flat-lagoon, tidal flat-delta, shallow water delta-lagoon, fluvial, and shallow water delta sedimentary environment, respectively (Shen et al., 2017 and 2018; Xie et al., 2017). The Benxi-Shanxi Formations are coal-bearing layers with significant volumes of coalbed methane, tight sandstone gas, and shale gas. The Lower and Upper Shihezi Formations are important layers for tight sandstone gas

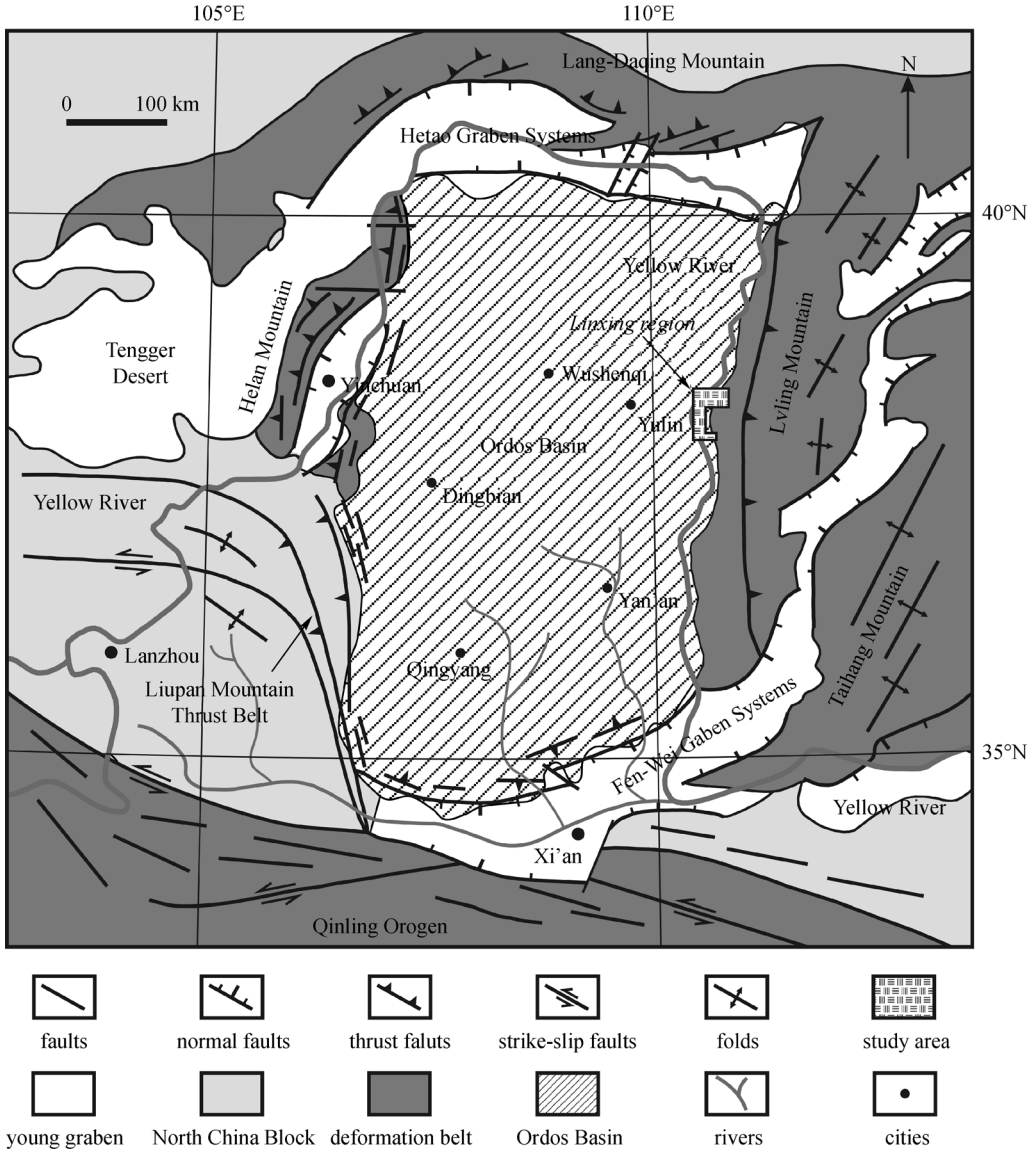

Fig. 2 Simplified regional geologic map of the Ordos Basin in central China.

production. Structures in the Linxing Block are relatively simple, and the stratigraphic strike is approximately NE-SW-trending and dips westward at 5°–10° (Ju et al., 2017; Gao et al., 2018).

3 Materials and methods

In this study, observations of natural fractures are mainly carried out based on outcrops, cores, and borehole image logs. The outcrops of gas-bearing formations are well exposed along the roads S248 and S218 in the study area, and the total length for natural fracture observations is approximately 3000 m long. Cores and borehole image logs are precise and quick methods for collecting subsurface fracture data. In this study, fracture descriptions from cores are performed in 13 vertical wells (~386.6 m). The borehole image logs contained Electrical Resistance Micro-Imaging (ERMI) from 8 wells, X-tended Range Micro-Imager (XRMI) from 3 wells and Electrical Micro-Imaging (EMI) from 1 well.

Detectable borehole fractures can be either natural in origin or induced by the drilling process. Hence, distinguishing natural from induced fractures should be first conducted during observations in cores and borehole image logs (Aadnoy and Bell, 1998; Rajabi et al., 2010; Qu et al., 2016; Ju et al., 2017). Within cores, induced fractures are easily determined by visually examining fracture surface morphology and the geometric relationships between the core and the fracture shape and propagation path (Nelson, 2001). Natural fracture surfaces are commonly regular and straight (Figs. 4(a) and 4(b)), and sometimes slickensides are present on natural fractures (Fig. 4(c)), whereas the surfaces of induced fractures are

Formation	Lithology description
Yanchang Formation	Upper: mudstone interbedded with fine sandstone and siltstone Lower: sandstone interbedded with purple mudstone
Zhifang Formation	Upper: gray-green mudstone and fine sandstone Lower: gray-green sandstone and conglomerate
Heshanggou Formation	Gray-green and maroon mudstone, light gray and maroon fine sandstone, interbedded with sandy mudstone
Liujiagou Formation	Fuchsia mudstone and siltstone, gray-brown fine sandstone, interbedded with thin maroon sandy mudstone
Sunjiagou Formation	Fuchsia-gray mudstone, siltstone and fine sandstone, interbedded with pelitic sandstone and sandy mudstone
Upper Shihezi Formation	Light gray fine sandstone and gray-green mudstone interbedded with fuchsia and gray carbonaceous mudstone
Lower Shihezi Formation	Light gray medium-fine sandstone and gray mudstone interbedded with conglomeratic sandstone
Shanxi Formation	Dark gray-black mudstone, light gray medium-fine sandstone and siltstone, black coal and carbonaceous mudstone
Taiyuan Formation	Dark gray-black carbonaceous mudstone, black coal, light gray medium-fine sandstone and siltstone
Benxi Formation	Dark gray mudstone and light gray fine sandstone interbedded with thin black coal
Majiagou Formation	Light gray dolomite

(a)

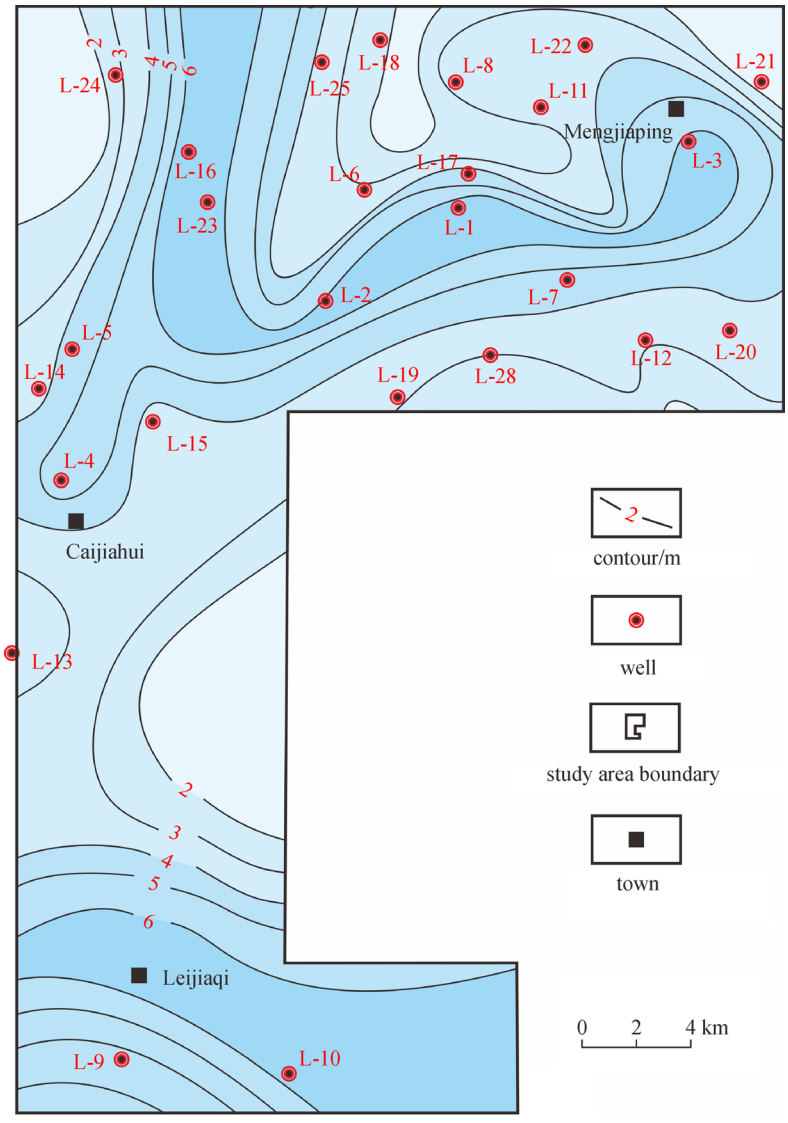

(b)

Fig. 3 Generalized stratigraphy (a) and well locations (b) in the Linxing Block of eastern Ordos Basin. The key unconventional gas-bearing layers in the Linxing Block consist of the Upper Shihezi, Lower Shihezi, Shanxi, Taiyuan and Benxi Formations (yellow in Fig. 3 (a)). The contours in Fig. 3(b) indicate coal thickness of the Shanxi Formation. The stratigraphic and petrographic data are after Gao et al. (2018) and Shu et al. (2019).

irregular with various shapes (Fig. 4(d)).

In electrical borehole image logs, conductive and resistive materials are coded in dark and bright colors, respectively (Canady and Market, 2008; Folkestad et al., 2012). Fractures can be identified when they are filled with electrically contrasting fluids or solids. Generally, on unrolled images, open natural fractures have conductive appearances with sinusoidal traces (Fig. 5(a)), partially filled fractures exhibit dark traces with bright traces. As to induced fractures, they appear in two different manners (Aadnoy and Bell, 1998; Zoback et al., 2003; Tingay et al., 2008; Ju et al., 2017), namely, 1) type I, they are symmetrically aligned two vertical/sub-vertical fractures parallel to the borehole axis on the opposite sides of the borehole wall (Fig. 5(b)), and 2) type II, they are en-echelon fractures around the borehole, exhibiting traces 180° apart at the borehole surface and inclined relative to the borehole axis (Fig.5(c)).

Parameters, commonly used for characterizing natural fractures, include the fracture aperture, filling, type, orientation, and density, etc (Nelson, 2001; Ju and Sun, 2016). The fracture aperture (or the fracture width), which is defined as the average distance between two subparallel fracture walls (van Golf-Racht, 1982; Marrett et al., 1999). According to the fracture aperture and filling, natural fractures are divided into four types: open fracture, partially open fracture without fillings, partially open fracture with fillings, and closed fracture. The fracture

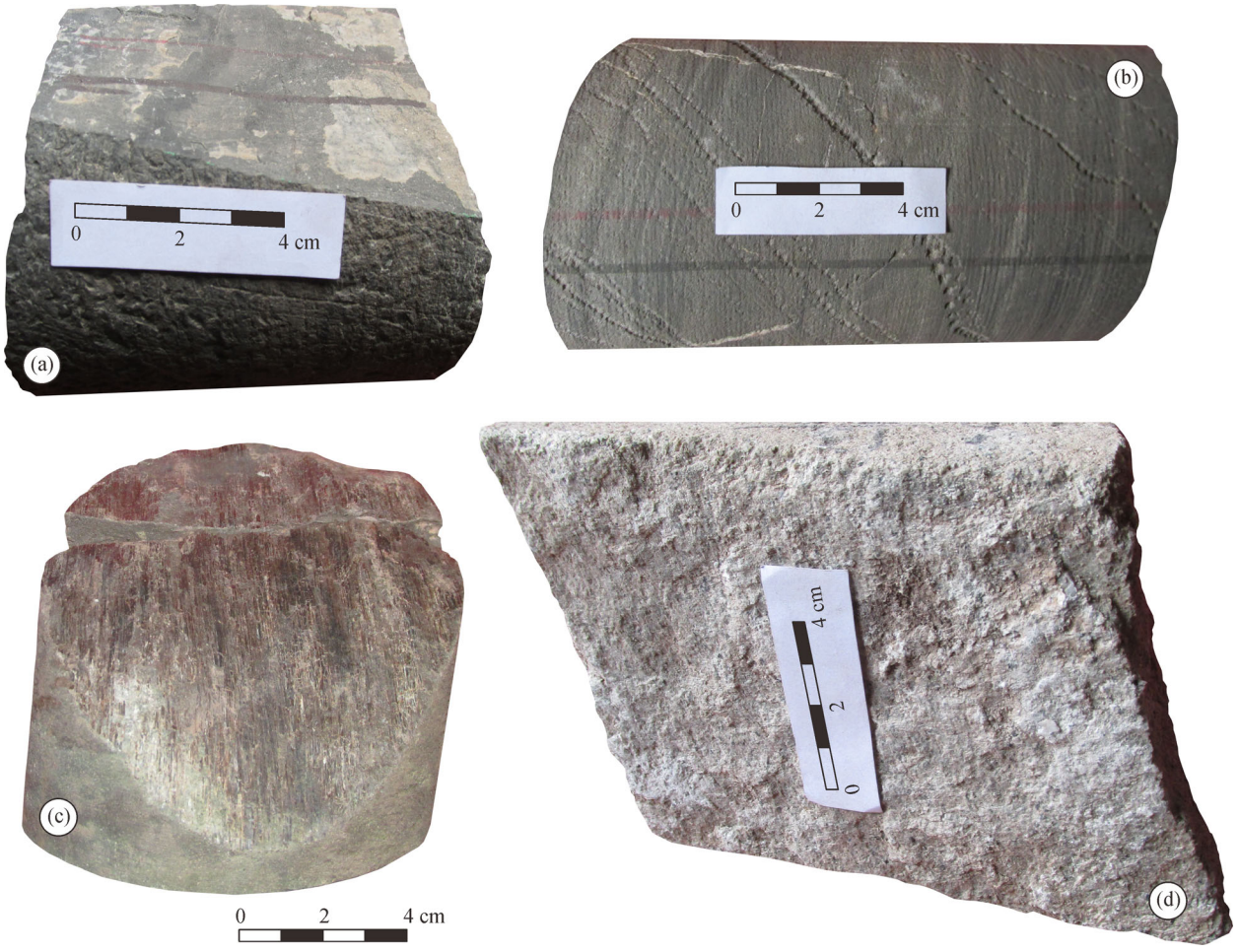

Fig. 4 Natural and induced fractures detected from cores in the Linxing Block of eastern Ordos Basin. (a) Well L-18, 1688.61 m, the Taiyuan Formation, (b) Well L-19, 1892.63 m, the Taiyuan Formation, (c) Well L-6, 1608.82 m, the Upper Shihezi Formation, and (d) Well L-18, 1355.13 m, the Lower Shihezi Formation.

orientation is determined by the strike and dip angle of a fracture plane. Based on dip angles of natural fractures, natural fractures have types of bedding fracture (0–15°), low-angle oblique fracture (15°–45°), high-angle oblique fracture (45°–75°), and vertical fracture (75°–90°) (Wang, 1992). The fracture density, including the linear fracture density, areal fracture density, and volumetric fracture density, represents the development degree of natural fractures (van Golf-Racht, 1982). In this study, the weighted areal fracture density is calculated based on Eqs. (1) and (2) to characterize natural fracture development.

$$d_{\mathrm{af}} = \frac{\Sigma_{i=0}^{n} L_i}{S}, \tag{1}$$

$$D_{\mathrm{waf}} = \frac{\Sigma_{j=0}^{m} (d_{\mathrm{af}j} \times h_j)}{T}, \tag{2}$$

where d_{af} is the areal fracture density in a single core rock, m^{-1}; L is the circumference of a single fracture in core rocks, m; S is the surface area of a single core rock, m^2; n is the total number of fractures in a single core rock, unitless; m is the total number of core rocks in a given formation, unitless; D_{waf} is the weighted areal fracture density, m^{-1}; h is the length of a single core rock, m; and T is the thickness of a given formation, m.

In the outcrops, some fractures are generally developed due to unloading, stress relaxation, and erosion; therefore, data from analogous outcrops are not used for characterizing fracture density and aperture. In the cores, the apparent apertures, dip angles, fillings and circumferences of natural fractures are observed and systematically measured, and hence, the weighted fracture densities in different gas-bearing formations are calculated. Characteristics of fracture orientation are mainly analyzed based on borehole imaging logs.

4 Characteristics of natural fractures

4.1 Fracture orientation

In the Linxing Block, based on the observations of natural

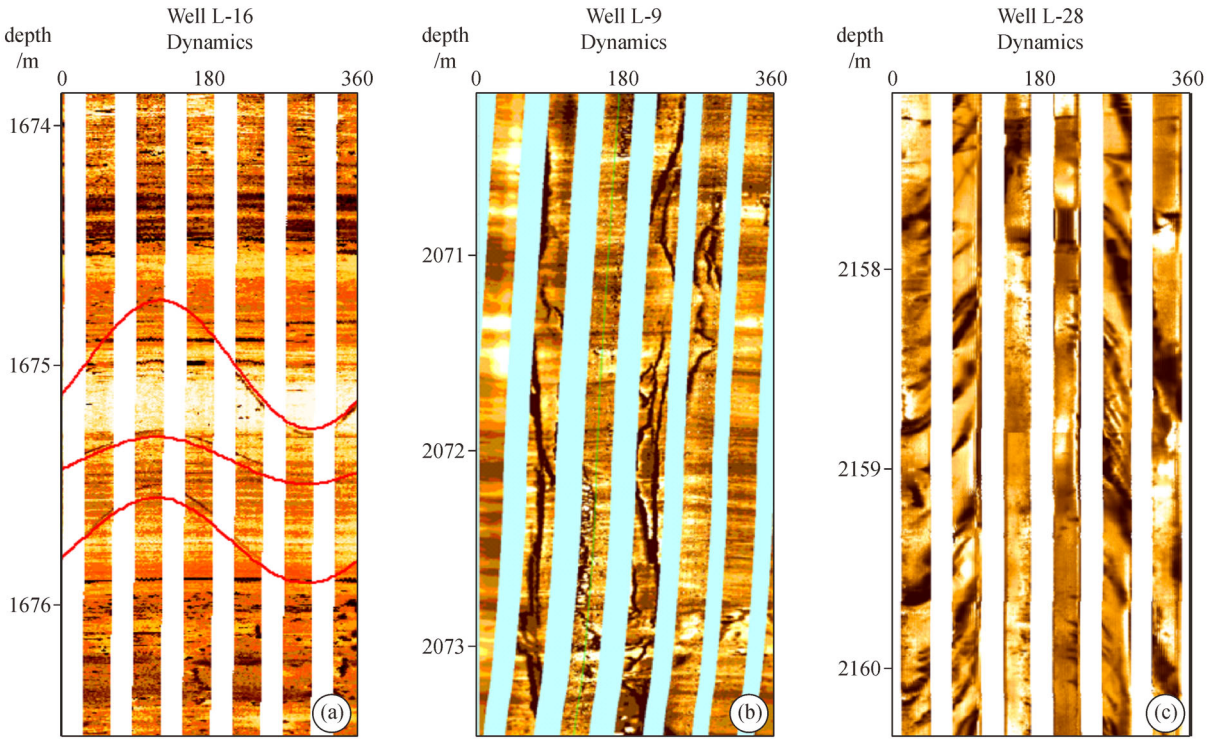

Fig. 5 Natural and induced fractures detected from borehole image logs in the Linxing Block of eastern Ordos Basin. (a) natural fracture, (b) induced fracture type I, and (c) induced fracture type II.

fractures from cores, 368 natural fractures are determined within the Benxi-Upper Shihezi Formations, among which, approximately 45.87% of them are high-angle oblique fractures. In addition, the following phenomena can also be observed: high-angle oblique fractures and vertical fractures are the dominant types in the Benxi-Shanxi coal-bearing formations; whereas the majority of natural fractures are high-angle and low-angle oblique fractures in the Lower and Upper Shihezi Formations (Fig.6).

Based on observations from outcrops and borehole image logs, the strikes of natural fractures in the Linxing Block are measured and plotted with rose diagrams (Fig.7), from which three sets of natural fractures can be detected, namely, the dominant ~N-S-trending (set I), WNW-ESE-trending (set II), and NE-SW-trending (set III).

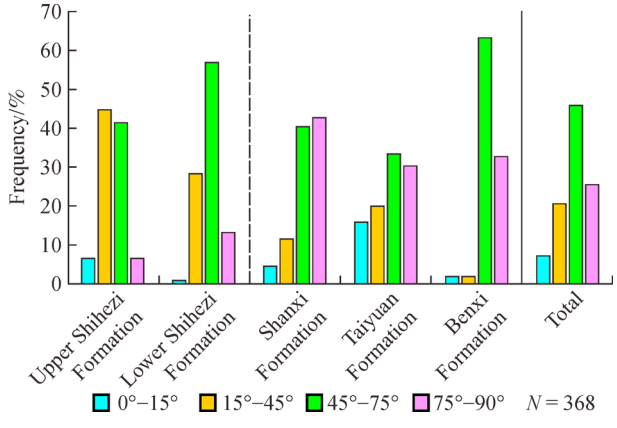

Fig. 6 Dip angles of natural fractures in the Linxing Block of eastern Ordos Basin.

4.2 Fracture aperture and fillings

Fracture aperture is defined as the distance between fracture walls, which mainly depends on rock lithological-petrographic characteristics and local stress state (van Golf-Racht, 1982; Wang, 1992; Gale et al., 2014). Furthermore, the real fracture aperture is difficult to obtain underground. The measured data from cores are generally larger, hence, a correction is required, which can be expressed as follows:

$$b = b_s \cos\alpha, \tag{3}$$

where b and b_s are real and apparent fracture aperture, mm; α is the angle between the measuring plane and fracture plane, degree.

In the Linxing Block, based on measurements and correction from cores, the majority of natural fracture in the Benxi-Upper Shihezi Formations indicate relatively small apertures, generally less than 2.0 mm. Especially in the Lower and Upper Shihezi Formations, all the investigated natural fractures have apertures less than 1.0 mm (Fig.8).

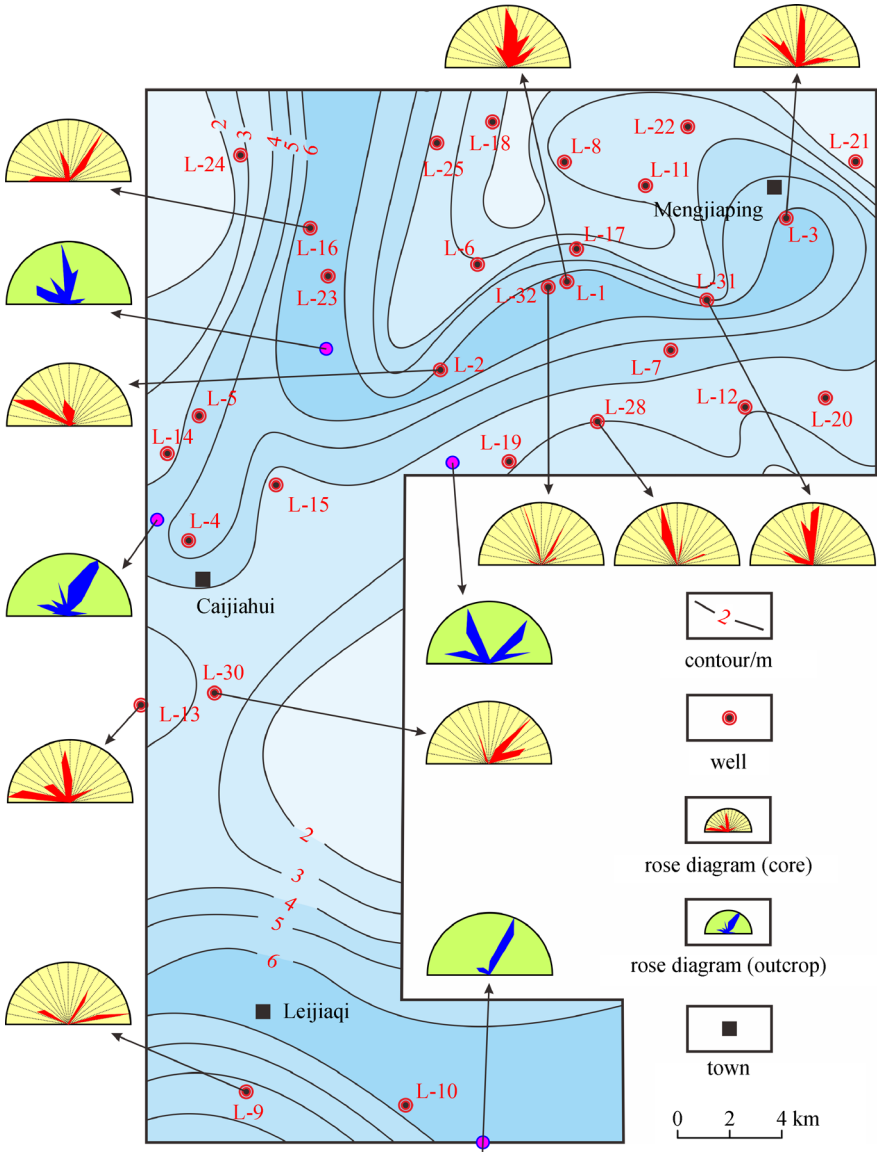

Fig. 7 Strike rose diagrams of natural fractures in the Linxing Block of eastern Ordos Basin (some data are from Gao et al. (2018)).

4.3 Fracture fillings

In this study, natural fractures are divided into open fracture, partially open fracture without fillings, partially open fractures with fillings, and closed fracture based on the filling condition of fractures. Among the investigated 368 natural fractures from cores in the Linxing Block, 64.36% of them belong to the type of open fracture, especially for those in the Lower and Upper Shihezi Formations (Fig. 9), which suggests that natural fractures may have favorable contributions to gas production. The minerals for those closed fractures are mainly calcite.

4.4 Fracture density

In the Linxing Block, measurements of natural fractures from cores and image logs indicate that natural fractures develop in all the Benxi-Upper Shihezi gas-bearing formations (Table 1). However, due to different factors, the weighted fracture densities vary in a broad scale, ranging between 0.002 m^{-1} (the Upper Shihezi Formation in Well L-23) and 0.565 m^{-1} (the Taiyuan Formation in Well L-19), which demonstrates the strong anisotropy of natural fractures within the gas-bearing formations of Linxing Block.

5 Discussions

5.1 Genesis analysis for natural fractures

During the Mesozoic and Cenozoic periods, structural features and characteristics of natural fractures in the eastern Ordos Basin are mainly influenced by the

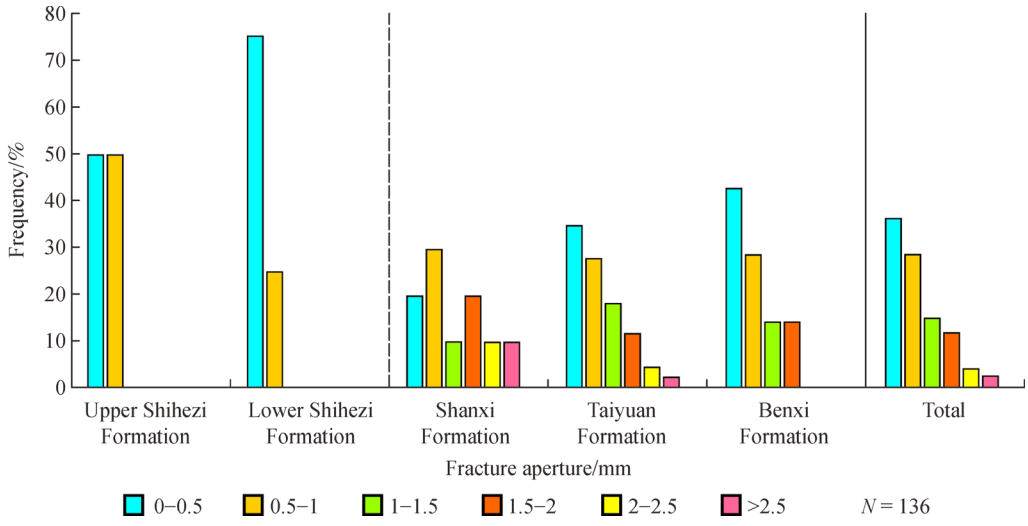

Fig. 8 Apertures of natural fractures in the Linxing Block of eastern Ordos Basin.

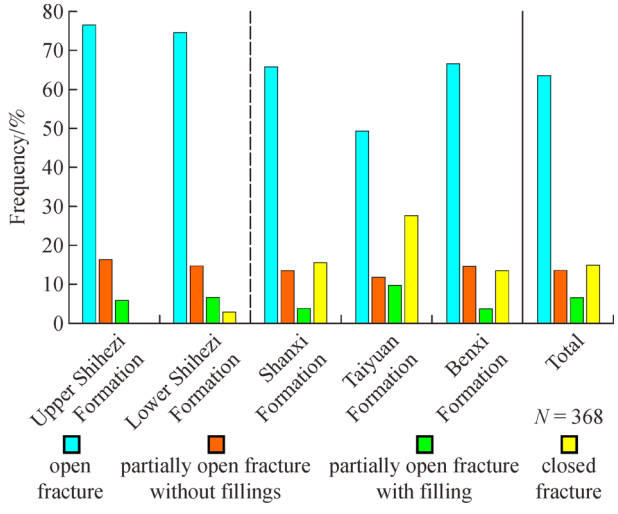

Fig. 9 Types of natural fractures based on fracture aperture and fillings in the Linxing Block of eastern Ordos Basin.

Indosinian, Yanshanian, and Himalayan movements. Among them, the Yanshanian tectonic stress field is critical for the Linxing Block because the dominant structural styles were basically formed and determined during that period (Wang et al., 2010).

Based on the interpretation of conjugate fractures in the outcrops, Gao et al. (2018) studied the paleo-tectonic stress fields in the Linxing Block. During the Yanshanian period, resulting from the far-field effects produced by subduction of the Paleo-pacific plate beneath the Asian continent (Wang et al., 2010), the study area was subjected to the NW-SE-trending horizontal tectonic compression. Under this stress condition, rocks were ruptured and natural fractures with ~NNW-SSE-trending and WNW-ESE-trending were generated. During the Himalayan period, as a result of the far-field effects from the collision between the Indian plate and the Eurasian plate (Wang et al., 2010), the horizontal tectonic compression was changed to NE-SW-trending in the Linxing Block, and natural fractures with ~NNE-SSW-trending and ENE-WSW-trending were hence formed.

5.2 Effects of lithology and layer thickness on natural fractures

In the Linxing Block, based on the measurements and statistics of natural fractures in cores, the development of natural fractures indicates a great deal of variability among different lithologies. The calculated fracture densities in different lithologies follow the order of carbonate rocks > coal > detrital rocks (Fig.10), which may possibly account for the higher fracture development in the Benxi-Shanxi Formations (Table 1). The Lower and Upper Shihezi Formations mainly consist of detrital rocks without coals and limestones (Fig.3). In addition, for detrital rock series, more natural fractures develop within siltstones and fine sandstones, whereas the fracture density is relatively low in coarse sandstones and mudstones.

The above phenomena may be possibly explained as follows. More natural fractures are developed in carbonate rocks than detrital rocks, which may result from the difference in their mineral compositions. Commonly, an increase in the proportion of brittle minerals will decrease the tensile strength and facilitate the generation of natural fractures under the same stress conditions (Bowker, 2007; Buller et al., 2010; Gale et al., 2014; Ju and Sun, 2016). In coals, cleats, a type of natural opening-mode fracture, are well developed and widely distributed (Laubach et al., 1998), causing relatively higher fracture densities. For the sandstone group, the rocks may become tighter with the decrease of particle size; hence, they will easily fail under low strain conditions after the elastic deformation stage

Table 1 The weighted natural fracture densities in different gas-bearing fromations of Linxing Block

Well / Fracture density /m^{-1} / Formation	L-1	L-5	L-6	L-12	L-15	L-18	L-19	L-20	L-21	L-22	L-23	L-24	L-25	average
Upper Shihezi	/	/	0.019	0.046	/	/	/	0.014	0.004	0.008	0.002	/	/	0.016
Lower Shihezi	0.032	/	0.015	0.016	/	0.072	0.004	0.007	0.004	/	0.049	0.046	/	0.027
Shanxi	0.094	0.015	/	/	0.017	0.040	0.075	/	0.012	/	/	0.038	0.019	0.039
Taiyuan	0.281	/	0.075	/	/	0.094	0.565	0.073	0.068	/	0.115	0.019	/	0.161
Benxi	0.160	/	/	0.214	/	/	/	0.015	0.120	/	/	/	/	0.127

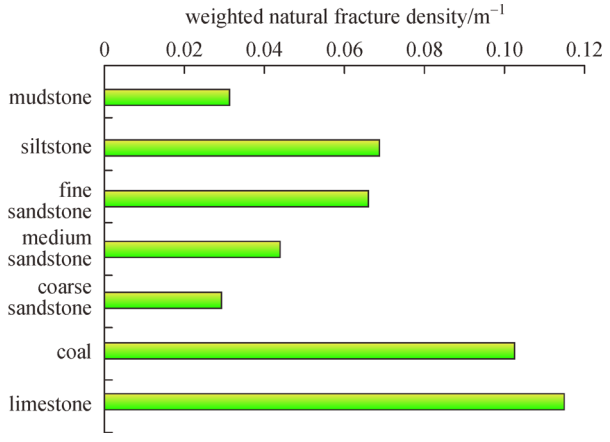

Fig. 10 The weighted natural fracture densities in different lithologies of Linxing Block.

(Zeng, 2008).

Under the same lithology and tectonic condition, observations in the outcrops of Linxing Block indicate that the fracture density decreases in some fashion with the thickness increase of a sedimentary layer (Fig. 11). Compared to thick ones, thin layers generally develop more natural fractures. It has been verified that this phenomenon applies to the majority of sedimentary rocks (Narr and Suppe, 1991; Nelson, 2001; Zeng, 2008).

5.3 Coupling effects of stress and pore pressure on natural fractures

Based on the interpretations from borehole breakouts (BOs) and drilling-induced tensile fractures (DITFs), Ju et al. (2017) analyzed the present-day *in-situ* stress state in the Linxing Block, and the results indicated that the horizontal maximum principal stress (S_{Hmax}) orientation was approximately E-W-trending.

In this study, no detailed production data were available, and hence the productivity of natural fractures was unable to be assessed. However, according to the stress and fracture orientations, only set II may be genetically linked to the present-day stress orientation, while the other two sets (set I and III) are oriented at a relatively high angle to the S_{Hmax} orientation. Hence, those natural fractures within set II belong to "stress-sensitive fractures" (Sibson, 1996; Rajabi et al., 2010), and may tend to be open and conductive under the present-day in-situ stress state.

To better understand the effects of present-day *in-situ* stresses on natural fractures, the Coulomb failure mechanism is introduced in this study. Natural fractures from the

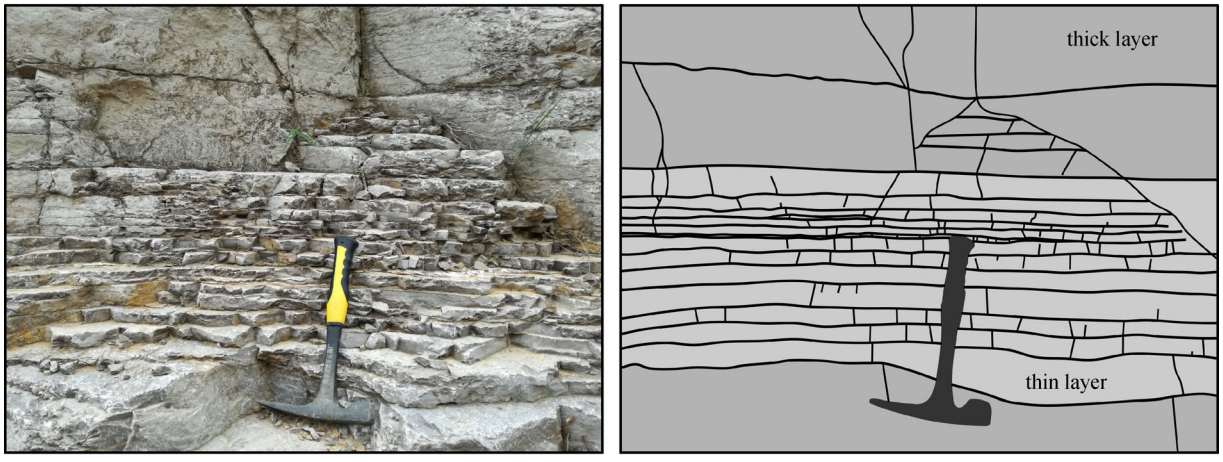

Fig. 11 Interpretation of natural fractures from a sandstone geological section in the Linxing Block.

Shanxi and Taiyuan Formations in Well L-1 are selected for analysis, and their orientations are interpreted from image logs and plotted in Fig. 12.

A standard frictional coefficient value of 0.6 is set to the cohesionless natural fractures. The present-day *in-situ* stress state is based on previous studies from Ju et al. (2017). The results indicate that all natural fractures from the Shanxi and Taiyuan Formations are obviously not critically stressed under the present-day *in-situ* stress state (Fig. 13). However, with pore pressure increases, ENE-WSW-trending fractures initially become critically stressed, and when the increased pore pressure is 4 SG, all natural fractures from the Shanxi Formation are critically stressed. During the whole process, natural fractures from the Taiyuan Formation are less likely to be critically stressed due to their ~N-S-trending orientations (Fig. 13).

Hence, though more fractures are developed in the Taiyuan Formation (Fig. 12), they are unlikely to become critically stressed. Because the production of unconventional gas requires hydraulic fracturing, the effectiveness of natural fractures under the present-day stress state may be more important for high production.

6 Conclusions

Understanding the development and distribution of natural fractures well in unconventional reservoirs is of great importance for gas production. In this study, characteristics and influencing factors for natural fractures in the Linxing Block were analyzed. The main results are described below.

1) Based on the calculated fracture density, the Benxi-Upper Shihezi gas-bearing formations indicate differential fracture development. Fracture orientation analysis shows that three sets of natural fractures can be detected in the Linxing Block, namely, ~N-S-trending, WNW-ESE-trending and NE-SW-trending. Approximately 45.87% of all natural fractures in the Benxi-Upper Shihezi Formations are high-angle oblique fractures. The majority of natural fractures are unfilled and belong to the open fracture type.

2) According to the characteristics of fracture sets and tectonic evolution of the study area, natural fractures are mainly formed in the Yanshanian and Himalayan periods. Fractures with ~NNW-SSE-trending and WNW-ESE-trending, ~NNE-SSW-trending and ENE-WSW-trending were generated during the Yanshanian period and

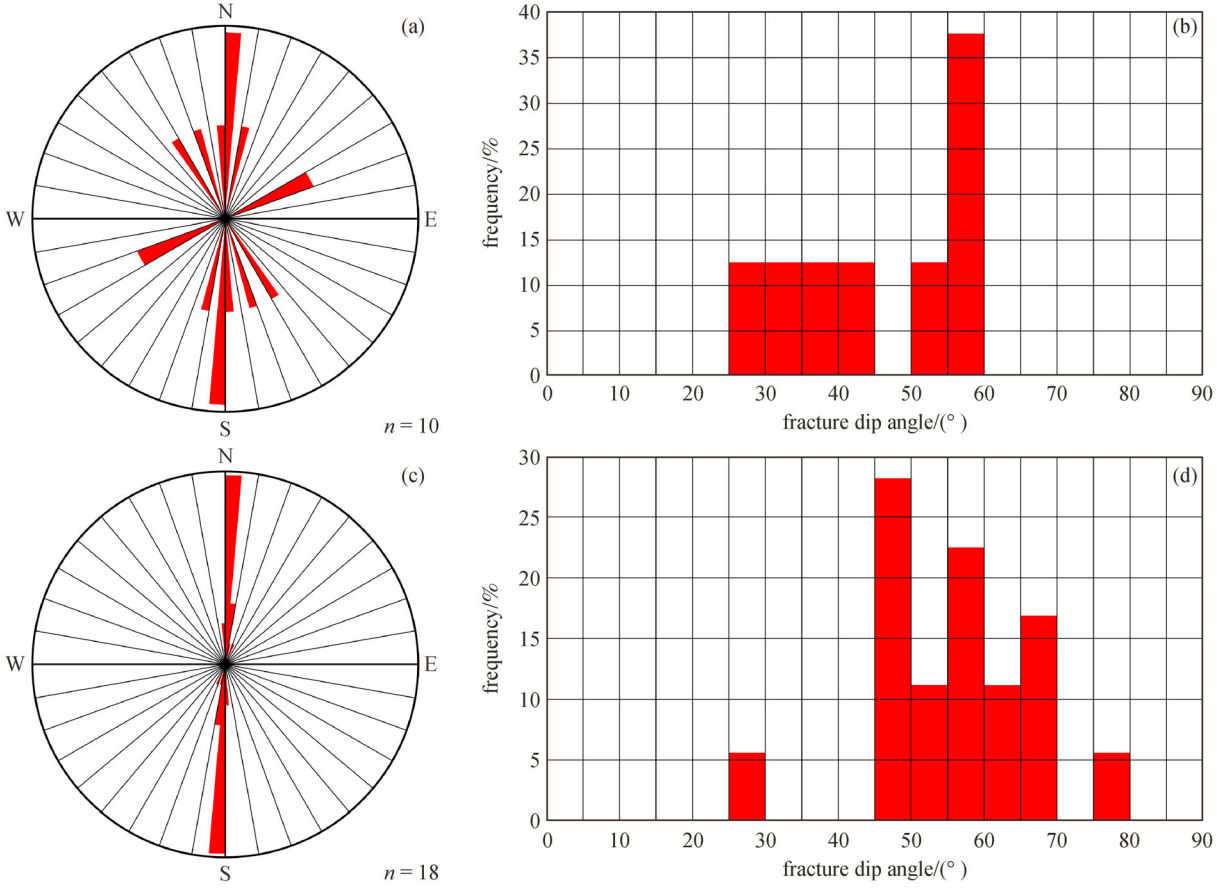

Fig. 12 Natural fractures interpreted from borehole image logs in the Shanxi and Taiyuan Formations of Well L-1 in the Linxing Block. (a) fracture dips from the Shanxi Formation, (b) fracture dip angles from the Shanxi Formation, (c) fracture dips from the Taiyuan Formation and (d) fracture dip angles from the Taiyuan Formation.

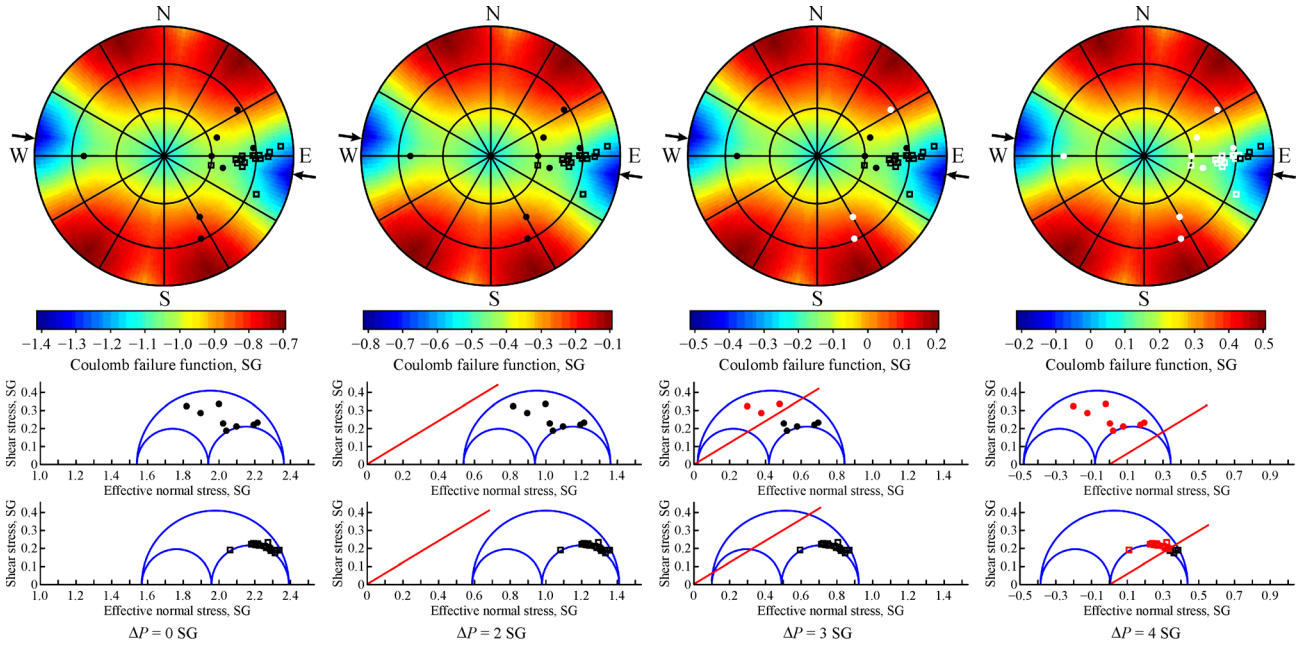

Fig. 13 Lower hemisphere stereonet plots and three-dimensional Mohr circles showing critically stressed natural fractures in the Shanxi and Taiyuan Formations of Well L-1, Linxing Block of eastern Ordos Basin. In stereonet plots, black data are normal fractures, and white ones are critically stressed fractures. In Mohr circles, black data are normal fractures, and red ones are critically stressed fractures. Dots and squares are those fractures from the Shanxi Formation and Taiyuan Formation, respectively. SG is specific gravity, g/cm^3. *ΔP* indicates the pore pressure increase.

Himalayan period, respectively.

3) The lithology and layer thickness influence the development of natural fractures. The calculated fracture densities in different lithologies of Linxing Block follow the order of carbonate rocks > coal > detrital rocks. More natural fractures are developed in thin sedimentary layers.

4) In the Linxing Block, ~N-S-trending fractures are difficult to critically stress, indicating that they contribute little to the subsurface fluid flow and further gas production.

Acknowledgements Many thanks to the financial support from National Natural Science Foundation of China (Grant Nos. 41702130 and 41872171), National Science and Technology Major Project (2016ZX05066), and Priority Academic Program Development of Jiangsu Higher Education Institutions (PAPD).

References

Aadnoy B S, Bell J S (1998). Classification of drilling-induced fractures and their relationship to in-situ stress directions. Log Anal, 39(6): 27–42

Aydin A (2000). Fractures, faults, and hydrocarbon entrapment, migration, and flow. Mar Pet Geol, 17(7): 797–814

Bhandakkar P, Siddhamshetty P, Sang-Il Kwon J (2020). Numerical study of the effect of propped surface area and fracture conductivity on shale gas production: application for multi-size proppant pumping schedule design. J Nat Gas Sci Eng, 79: 103349

Bowker K A (2007). Barnett shale gas production, Fort Worth Basin: issues and discussion. AAPG Bull, 91(4): 523–533

Buller D, Hughes S N, Market J, Petre J E, Spain D R, Odumosu T (2010). Petrophysical evaluation for enhancing hydraulic stimulation in horizontal shale gas wells. Society of Petroleum Engineers

Canady W, Market J, (2008). Fracture characterization by borehole logging methods. Society of Petrophysicists and Well-Log Analysts, SPWLA-2008-AAA (1–12)

Dahi-Taleghani A, Olson J E (2011). Numerical modeling of multi-stranded-hydraulic-fracture propagation: accounting for the interaction between induced and natural fractures. Society of Petroleum Engineers, 16(3): 575–581

Folkestad A, Veselovsky Z, Roberts P (2012). Utilising borehole image logs to interpret delta to estuarine system: a case study of the subsurface Lower Jurassic Cook Formation in the Norwegian northern North Sea. Mar Pet Geol, 29(1): 255–275

Fossen H (2010). Structural Geology. Cambridge: Cambridge University Press

Gale J F W, Laubach S E, Olson J E, Eichhuble P, Fall A (2014). Natural fractures in shale: a review and new observations. AAPG Bull, 98 (11): 2165–2216

Gale J F W, Reed R M, Holder J (2007). Natural fractures in the Barnett Shale and their importance for hydraulic fracture treatments. AAPG Bull, 91(4): 603–622

Gao X D, Wang Y B, Ni X M, Li Y, Wu X, Zhao S H, Yu Y (2018). Recovery of tectonic traces and its influence on coalbed methane reservoirs: a case study in the Linxing area, eastern Ordos Basin, China. J Nat Gas Sci Eng, 56: 414–427

Hall S A, Kendall J M, Barkved O I (2002). Fractured reservoir characterization using P-wave AVOA analysis of 3D OBC data.

Leading Edge (Tulsa Okla), 21(8): 777–781

Hancock P L (1985). Brittle microtectonics: principles and practice. J Struct Geol, 7(3–4): 437–457

Harstad H, Teufel L W, Lorenz J C (1995). Characterization and simulation of naturally fractured tight gas sandstones. Society of Petroleum Engineers

Hennings P H, Olson J E, Thompson L B (2000). Combining outcrop data and three-dimensional structural models to characterize fractured reservoir: an example from Wyoming. AAPG Bull, 84: 830–849

Ju W, Niu X B, Feng S B, You Y, Xu K, Wang G, Xu H R (2020). Present-day *in-situ* stress field within the Yanchang Formation tight oil reservoir of Ordos Basin, central China. J Petrol Sci Eng, 187: 106809

Ju W, Shen J, Qin Y, Meng S Z, Wu C F, Shen Y L, Yang Z B, Li G Z, Li C (2017). *In-situ* stress state in the Linxing region, eastern Ordos Basin, China: implications for unconventional gas exploration and production. Mar Pet Geol, 86: 66–78

Ju W, Sun W F (2016). Tectonic fractures in the Lower Cretaceous Xiagou Formation of Qingxi Oldfield, Jiuxi Basin, NW China. Part one: characteristics and controlling factors. J Petrol Sci Eng, 146: 617–625

Ju W, Sun W F, Hou G T (2015). Insights into the tectonic fractures in the Yanchang Formation interbedded sandstone-mudstone of the Ordos Basin based on core data and geomechanical models. Acta Geol Sin, 89(6): 1986–1997

Ju W, Wang J L, Fang H H, Sun W F (2019). Paleotectonic stress field modeling and prediction of natural fractures in the Lower Silurian Longmaxi shale reservoirs, Nanchuan region, South China. Mar Pet Geol, 100: 20–30

Ju W, Wang K, Hou G T, Sun W F, Yu X (2018). Prediction of natural fractures in the Lower Jurassic Ahe Formation of the Dibei Gasfield, Kuqa Depression, Tarim Basin, NW China. Geosci J, 22(2): 241–252

Laubach S E, Marrett R A, Olson J E, Scott A R (1998). Characteristics and origins of coal cleat: a review. Int J Coal Geol, 35(1–4): 175–207

Laubach S E, Olson J E, Gross M R (2009). Mechanical and fracture stratigraphy. AAPG Bull, 93(11): 1413–1426

Li Y, Tang D Z, Wu P, Niu X L, Wang K, Qiao P, Wang Z S (2016). Continuous unconventional natural gas accumulation of Carboniferous-Permian coal-bearing strata in the Linxing area, northeastern Ordos Basin, China. J Nat Gas Sci Eng, 36: 314–327

Liu C Y, Zhao H G, Sun Y Z (2009). Tectonic background of Ordos Basin and its controlling role for basin evolution and energy mineral deposits. Energy Exploration and Exploitation, 27(1): 15–27

Marrett R, Ortega O J, Kelsey C M (1999). Extent of power-law scaling for natural fractures in rock. Geology, 27(9): 799–802

McGinnis R N, Ferrill D A, Morris A P, Smart K J, Lehrmann D (2017). Mechanical stratigraphic controls on natural fracture spacing and penetration. J Struct Geol, 95: 160–170

Narr W (1991). Fracture density in the deep subsurface: techniques with application to Point Arguello Oil Field. AAPG Bull, 75: 1300–1323

Narr W, Suppe J (1991). Joint spacing in sedimentary rocks. J Struct Geol, 13(9): 1037–1048

Nelson R A (2001). Geologic Analysis of Naturally Fractured Reservoirs. 2nd ed. Massachusetts: Gulf Professional Publishing

Olson J E, Laubach S E, Lander R H (2009). Natural fracture characterization in tight gas sandstones: integrating mechanics and diagenesis. AAPG Bull, 93(11): 1535–1549

Qu H Z, Zhang F X, Wang Z Y, Yang X T, Liu H T, Ba D, Wang X (2016). Quantitative fracture evaluation method based on core-image logging: a case study of Cretaceous Bashijiqike Formation in ks2 well area, Kuqa depression, Tarim Basin, NW China. Pet Explor Dev, 43(3): 465–473

Rajabi M, Sherkati S, Bohloli B, Tingay M (2010). Subsurface fracture analysis and determination of in-situ stress direction using FMI logs: an example from the Santonian carbonates (Ilam Formation) in the Abadan Plain, Iran. Tectonophysics, 492(1–4): 192–200

Sibson R H (1996). Structural permeability of fluid-driven fault-fracture meshes. J Struct Geol, 18(8): 1031–1042

Shen J, Qin Y, Zhang B, Li G Z, Shen Y L (2018). Superimposing gas-bearing system in coal measures and its compatibility in Linxing block, east Ordos Basin. Journal of China Coal Society, 43(6): 1614–1619 (in Chinese)

Shen Y L, Qin Y, Wang G, Guo Y H, Shen J, Gu J Y, Xiao Q, Zhang T, Zhang C L, Tong G C (2017). Sedimentary control on the formation of a multi-superimposed gas system in the development of key layers in the sequence framework. Mar Pet Geol, 88: 268–281

Shu Y, Lin Y X, Liu Y, Yu Z Y (2019). Control of magmatism on gas accumulation in Linxing area, Ordos Basin, NW China: evidence from fluid inclusions. J Petrol Sci Eng, 180: 1077–1087

Siddhamshetty P, Bhandakkar P, Kwon J S (2020). Enhancing total fracture surface area in naturally fractured unconventional reservoirs via model predictive control. J Petrol Sci Eng, 184: 106525

Speight J G (2019). Natural Gas: A Basin Handbook. 2nd ed. Massachusetts: Gulf Professional Publishing

Tingay M, Reinecker J, Muller B, (2008). Borehole breakout and drilling-induced fracture analysis from image logs. World Stress Map Project Guidelines: Image Logs, 1–8

van Golf-Racht T D (1982). Fundamentals of Fractured Reservoir Engineering. New York: Elsevier Scientific Publishing Company

Wang X Y, Zhang Q L, Wang L S, Ge R F, Chen J (2010). Structural features and tectonic stress fields of the Mesozoic and Cenozoic in the eastern margin of the Ordos Basin. Geological Bulletin of China, 29 (8): 1168–1176 (in Chinese)

Wang Y C (1992). Fractured Tight Oil and Gas Reservoirs. Beijing: Geological Publishing House

Weniger S, Weniger P, Littke R (2016). Characterizing coal cleats from optical measurements for CBM evaluation. Int J Coal Geol, (154–155): 176–192

Wu K, Olson J E (2016). Numerical investigation of complex hydraulic-fracture development in naturally fractured reservoirs. SPE Prod Oper, 31(4): 300

Xie Y G, Sun X Y, Wan H, Duan C J, Chen Q, Yu Y J (2017). A study of shallow-water deltaic facies from Upper Shihezi Formation in Linxing area, Ordos Basin. Unconventional Oil and Gas, 4(2): 13–21 (in Chinese)

Yang Y T, Li W, Ma L (2005). Tectonic and stratigraphic controls of hydrocarbon systems in the Ordos Basin: a multicycle cratonic basin in central China. AAPG Bull, 89(2): 255–269

Zeng L B (2008). Formation and Distribution of Natural Fractures in Low-permeability Sandstone Reservoirs. Beijing: Science Press (in

Chinese)

Zeng L B, Li X Y (2009). Fractures in sandstone reservoirs with ultra-low permeability: a case study of the Upper Triassic Yanchang Formation in the Ordos Basin, China. AAPG Bull, 93(4): 461–477

Zhao G C, Sun M, Wilde S A, Li S Z (2005). Late Archean to Paleoproterozoic evolution of the North China Craton: key issues revisited. Precambrian Res, 136(2): 177–202

Zhao M W, Hans J B, Hans A (1996). Thermal and tectonic history of the Ordos Basin, China: Evidence from apatite fission track analysis, vitrinite reflectance, and K-Ar dating. AAPG Bull, 80(7): 1110–1134

Zoback M D, Barton C A, Brudy M, Castillo D A, Finkbeiner T, Grollimund B R, Moos D B, Peska P, Ward C D, Wiprut D J (2003). Determination of stress orientation and magnitude in deep wells. Int J Rock Mech Min Sci, 40(7–8): 1049–1076